

Higher order corrections to H^\pm production

Nikolaos Kidonakis^{*†}

Kennesaw State University, USA

E-mail: nkidonak@kennesaw.edu

I discuss recent calculations of higher-order corrections to charged Higgs production through various partonic subprocesses. Particular attention is paid to H^- production in association with a top quark at the LHC.

Prospects for Charged Higgs Discovery at Colliders
16-19 September 2008
Uppsala, Sweden

^{*}Speaker.

[†]This work was supported by the National Science Foundation under Grant No. PHY 0555372.

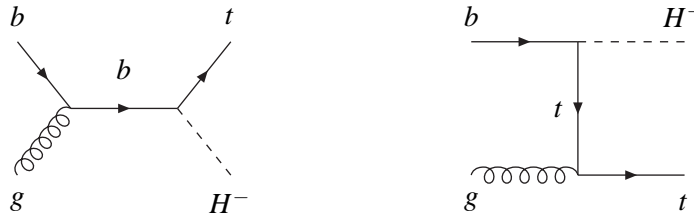


Figure 1: LO diagrams for $bg \rightarrow tH^-$.

1. Introduction

Many models for new physics involve a more complicated Higgs sector than in the Standard Model. In the Minimal Supersymmetric Standard Model (MSSM) and other two-Higgs-doublet models (2HDM), one Higgs doublet gives mass to the up-type fermions and the other to the down-type fermions, with $\tan\beta = v_2/v_1$ the ratio of the vacuum expectation values for the two doublets. The five physical Higgs particles in the MSSM include a light scalar, h^0 , a heavy scalar, H^0 , a pseudoscalar, A^0 , and two charged Higgs bosons, H^+ and H^- . A future discovery of a charged Higgs boson would constitute a definite sign of new physics. The Large Hadron Collider (LHC) is well positioned for a discovery of a charged Higgs [1].

A lot of work on higher-order QCD and SUSY corrections to charged Higgs production has been performed over the last several years, including next-to-leading order (NLO) calculations for $bg \rightarrow tH^-$ [2, 3, 4], $b\bar{b} \rightarrow H^+W^-$ [5, 6], $b\bar{b} \rightarrow H^+H^-$ [7, 8], $q\bar{q} \rightarrow H^+H^-$ [8], as well as results for higher-order soft-gluon corrections for $bg \rightarrow tH^-$ [9, 10].

2. Associated H^- and top quark production

We begin with the dominant process at the LHC, which is associated charged Higgs and top quark production. The leading order (LO) process is $bg \rightarrow tH^-$ and the corresponding Feynman diagrams are shown in Fig. 1. The LO cross section is proportional to $\alpha\alpha_s(m_b^2 \tan^2\beta + m_t^2 \cot^2\beta)$ where m_b is the bottom quark mass and m_t is the top quark mass.

Yukawa and SUSY electroweak corrections for this process were calculated in [11] and 1-loop SUSY corrections in [12, 13]. The complete NLO QCD corrections were calculated in Ref. [2, 3, 4]. The QCD corrections were shown to be substantial, contributing up to 85% enhancement of the lowest order cross section [2], and to reduce the scale dependence of the cross section. The NLO SUSY-QCD corrections are smaller in comparison, with their precise value depending on MSSM parameters [3, 4].

To calculate the NLO QCD corrections, we have to include the one-loop virtual corrections to $bg \rightarrow tH^-$ and also the processes with one additional parton:

$$\begin{array}{llllll}
 bg \rightarrow tH^-g & gg \rightarrow tH^-b & q\bar{q} \rightarrow tH^-b & bq \rightarrow tH^-q & b\bar{q} \rightarrow tH^-q \\
 bb \rightarrow tH^-b & b\bar{b} \rightarrow tH^-b & & &
 \end{array}$$

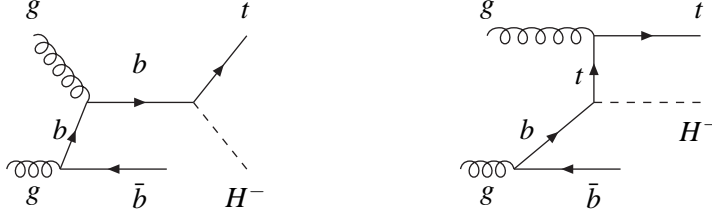


Figure 2: LO diagrams for $gg \rightarrow \bar{b}tH^-$ with a gluon splitting to $b\bar{b}$.

Issues with the calculation include the treatment of the bottom parton distribution, with a gluon splitting to $b\bar{b}$ in the collinear approximation, valid for small b -quark p_T . The diagrams for the process $gg \rightarrow \bar{b}tH^-$ with a gluon splitting to $b\bar{b}$ are shown in Fig. 2.

Work on matching the processes $bg \rightarrow tH^-$ and $gg \rightarrow \bar{b}tH^-$ [14] has been performed in [15, 16, 17]. The use of matrix elements at large p_T and parton showers at small p_T , results in double counting for small p_T when doing a simple addition. The matching performed in [17] involves an analytic double-counting subtraction term, and it can be implemented in event generators to give smooth differential distributions for all b -quark p_T .

2.1 $bg \rightarrow tH^-$ near threshold

Higher-order corrections to charged Higgs production near threshold have been calculated at next-to-next-to-leading order (NNLO) in Ref. [9] and at next-to-next-to-next-to-leading order (NNNLO) in Ref. [10].

For the process $b(p_b) + g(p_g) \rightarrow t(p_t) + H^-(p_H)$ we define the kinematical invariants $s = (p_b + p_g)^2$, $t = (p_b - p_t)^2$, $u = (p_g - p_t)^2$, and $s_4 = s + t + u - m_t^2 - m_H^2$, where m_t is the top quark mass and m_H is the charged Higgs mass. Note that, while we use the $\overline{\text{MS}}$ bottom quark mass in the coupling, we set $m_b = 0$ in the kinematics. At threshold $s_4 \rightarrow 0$, and the soft-gluon corrections take the form $[\ln^l(s_4/m_H^2)/s_4]_+$ and can be resummed. For the order α_s^n corrections $l \leq 2n - 1$. The leading logarithms (LL) are with $l = 2n - 1$ and the next-to-leading logarithms (NLL) are with $l = 2n - 2$.

Near threshold these soft-gluon corrections are dominant and provide good approximations to the complete QCD corrections. The NLO and NNLO soft-gluon corrections were calculated at NLL accuracy in [9]. Furthermore, the NNNLO soft NLL corrections were presented in [10].

The calculation of these corrections is derived from the fixed-order expansion of the resummed cross section. Resummation follows from factorization properties of the cross section and is performed in moment space. We can write the resummed cross section as [9, 10, 18]

$$\hat{\sigma}_{bg \rightarrow tH^-}^{res}(N) = \exp \left[\sum_i E_i(N_i) \right] \exp \left[\sum_i 2 \int_{\mu_f}^{\sqrt{s}} \frac{d\mu}{\mu} \gamma_{i/i}(N_i, \alpha_s(\mu)) \right] \exp \left[\sum_i 2 \int_{\mu_R}^{\sqrt{s}} \frac{d\mu}{\mu} \beta(\alpha_s(\mu)) \right] \\ \times H^{bg \rightarrow tH^-}(\alpha_s(\mu_R)) S^{bg \rightarrow tH^-}(\alpha_s(\sqrt{s}/\tilde{N})) \exp \left[\int_{\sqrt{s}}^{\sqrt{s}/\tilde{N}} \frac{d\mu}{\mu} 2\text{Re}\Gamma_S^{bg \rightarrow tH^-}(\alpha_s(\mu)) \right] \quad (2.1)$$

where the factorization scale is denoted by μ_F and the renormalization scale by μ_R , and N is the moment variable. In the numerical results later we will set these two scales equal to each other and denote them by μ . The first exponent in Eq. (2.1) is

$$\sum_i E_i(N_i) = -\sum_i C_i \int_0^1 dz \frac{z^{N_i-1} - 1}{1-z} \left\{ \int_{(1-z)^2}^1 \frac{d\lambda}{\lambda} \frac{\alpha_s(\lambda s)}{\pi} + \frac{\alpha_s((1-z)^2 s)}{\pi} \right\} + \mathcal{O}(\alpha_s^2) \quad (2.2)$$

with $C_i = C_F = (N_c^2 - 1)/(2N_c)$ for quarks and $C_i = C_A = N_c$ for gluons.

The second exponent in Eq. (2.1) involves the moment-space anomalous dimension $\gamma_{i/i}$ of the $\overline{\text{MS}}$ parton density, and the third exponent involves the QCD β function. $H^{bg \rightarrow tH^-}$ and $S^{bg \rightarrow tH^-}$ stand respectively for the hard-scattering function and the soft-gluon function. $\Gamma_S^{bg \rightarrow tH^-}$ is the soft anomalous dimension, and its explicit form at one loop for this process is

$$\Gamma_S^{bg \rightarrow tH^-} = \frac{\alpha_s}{\pi} \left[C_F \ln \left(\frac{-t + m_t^2}{m_t \sqrt{s}} \right) + \frac{C_A}{2} \ln \left(\frac{-u + m_t^2}{-t + m_t^2} \right) + \frac{C_A}{2} (1 - i\pi) \right] + \mathcal{O}(\alpha_s^2). \quad (2.3)$$

We then expand the moment-space expression of Eq. (2.1) for the resummed cross section through NNNLO and invert back to momentum space.

The NLO soft gluon corrections can be written as

$$\frac{d\hat{\sigma}^{(1)}(s_4)}{dt du} = F^B \frac{\alpha_s(\mu_R^2)}{\pi} \left\{ c_3 \left[\frac{\ln(s_4/m_H^2)}{s_4} \right]_+ + c_2 \left[\frac{1}{s_4} \right]_+ + c_1^\mu \delta(s_4) \right\} \quad (2.4)$$

with F^B the Born term, $c_3 = 2(C_F + C_A)$, and expressions for the other coefficients as given in [9, 10].

The NNLO soft gluon corrections are [9]

$$\frac{d\hat{\sigma}^{(2)}(s_4)}{dt du} = F^B \frac{\alpha_s^2(\mu_R^2)}{\pi^2} \left\{ \frac{1}{2} c_3^2 \left[\frac{\ln^3(s_4/m_H^2)}{s_4} \right]_+ + \left[\frac{3}{2} c_3 c_2 - \frac{\beta_0}{4} c_3 \right] \left[\frac{\ln^2(s_4/m_H^2)}{s_4} \right]_+ + \dots \right\} \quad (2.5)$$

where explicit expressions for subleading terms can be found in [9].

The NNNLO soft gluon corrections are [10]

$$\frac{d\hat{\sigma}^{(3)}(s_4)}{dt du} = F^B \frac{\alpha_s^3(\mu_R^2)}{\pi^3} \left\{ \frac{1}{8} c_3^3 \left[\frac{\ln^5(s_4/m_H^2)}{s_4} \right]_+ + \left[\frac{5}{8} c_3^2 c_2 - \frac{5}{24} \beta_0 c_3^2 \right] \left[\frac{\ln^4(s_4/m_H^2)}{s_4} \right]_+ + \dots \right\} \quad (2.6)$$

and explicit expressions for the subleading terms and further details are given in [10].

2.2 H^- production via $bg \rightarrow tH^-$ at the LHC

We now provide some numerical results for charged Higgs production in association with a top quark at the LHC.

We first show that the soft-gluon corrections are dominant by comparing the NLO-NLL results with the exact NLO results that have been derived in Ref. [2]. We note that in [2] the reference scale chosen was $\mu = m_H + m_t$. In most of the results below we will choose $\mu = m_H$, which is a natural choice in our calculation. A cross section known to all orders does not depend on the scale. However a finite-order cross section does depend on the scale, though the dependence decreases as we move from LO to NLO, NNLO, NNNLO and so on. The work in [2, 3] indeed showed

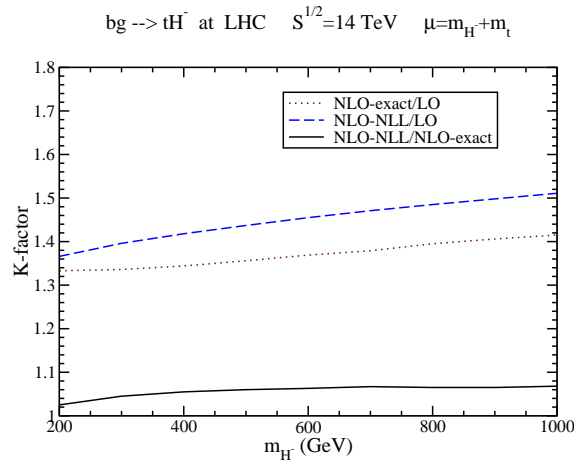


Figure 3: NLO exact and approximate K factors for H^- production at the LHC.

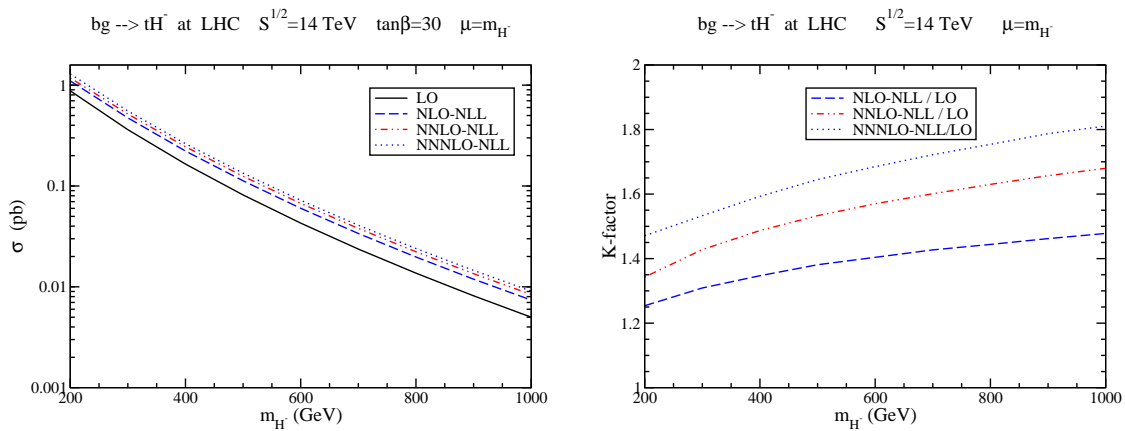
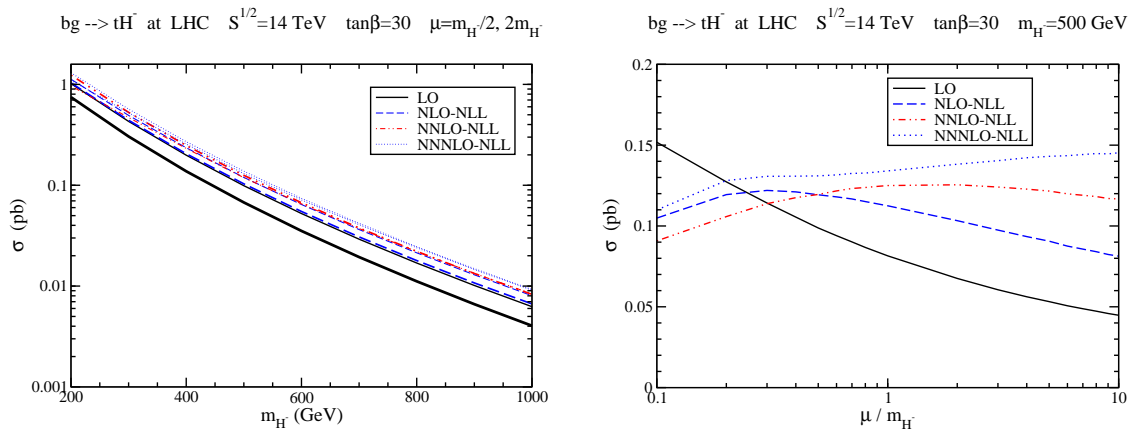


Figure 4: The total cross section (left) and K factors (right) for H^- production at the LHC.

a reduction of scale dependence when the NLO corrections are added relative to the LO cross section. In fact, as we will see below, the higher-order threshold corrections further decrease the scale dependence, thus resulting in more stable predictions. But to make the comparison to [2] we use a scale choice $\mu = m_H + m_t$ in Figure 3 and plot the K factors for H^- production at the LHC. The NLO-exact / LO curve shows the enhancement from the complete NLO corrections [2] while the NLO-NLL / LO curve shows the contribution of the NLL soft-gluon corrections at NLO. The two curves are close to each other and this is more easily seen from their ratio. The fact that the NLO-NLL / NLO-exact curve is very close to 1 (only a few percent difference) shows that the NLO-NLL cross section is a remarkably good approximation to the exact NLO result.

In Figure 4, on the left, we plot the cross section versus charged Higgs mass for pp collisions at the LHC with $\sqrt{s} = 14$ TeV using the MRST2002 approximate NNLO parton distributions functions [19] with a three-loop evaluation of α_s . We show results for the LO, NLO-NLL, and NNLO-NLL, and NNNLO-NLL cross sections, all with a choice of scale $\mu = m_H$ and with $\tan\beta =$

K factors		
m_H (GeV)	NNLO-NLL	NNNLO-NLL
200	1.34	1.47
300	1.43	1.53
400	1.49	1.59
500	1.53	1.65
600	1.57	1.69
700	1.60	1.72
800	1.63	1.75
900	1.66	1.79
1000	1.68	1.81

Table 1: The K factors for H^- production at the LHC.**Figure 5:** The scale dependence of the H^- cross section.

30. The cross section spans three orders of magnitude in the mass range $200 \text{ GeV} \leq m_H \leq 1000 \text{ GeV}$. The higher-order threshold corrections are positive and provide a significant enhancement to the lowest-order result. The cross sections for the related process $\bar{b}g \rightarrow \bar{t}H^+$ are exactly the same.

The right plot of Figure 4 shows the relative size of the corrections as K factors at $\mu = m_H$. The NLO-NLL / LO curve shows that the NLO-NLL soft corrections enhance the LO result by 25% to 48% depending on the charged Higgs mass. The K factors increase with higher masses, as expected, since then we get closer to threshold. With the NNLO-NLL corrections added we get an enhancement over the LO result of 34% to 68%. Adding further the NNNLO-NLL corrections provides an enhancement ranging from 47% to 81% over the LO result.

In Table 1 we show the explicit numbers for the NNLO-NLL and NNNLO-NLL K factors for specific values of the charged Higgs mass with $\mu = m_H$.

We next study the scale dependence of the cross section. On the left plot of Figure 5 we show the cross section at the LHC with $\tan\beta = 30$ as a function of charged Higgs mass with two different choices of scale, $\mu = m_H/2$ and $2m_H$. The scale variation of the LO cross section is quite large.

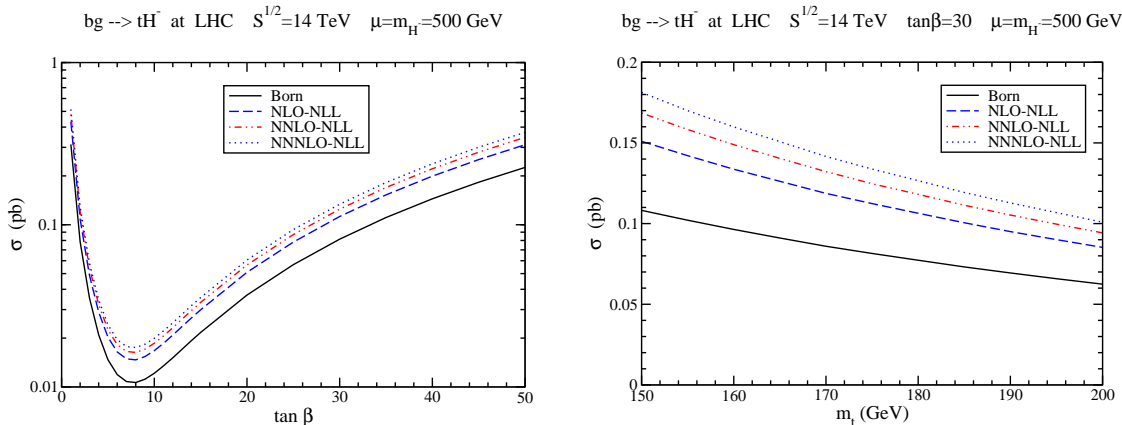


Figure 6: The $\tan\beta$ (left) and top mass (right) dependence of the H^- cross section.

The variation at NLO-NLL is smaller, and at NNLO-NLL and NNNLO-NLL it is very small. In fact the two NNLO-NLL curves are on top of each other for much of the range in m_H , as are the two NNNLO-NLL curves.

On the right plot of Figure 5, we show the scale dependence of the cross section for $m_H = 500$ GeV and $\tan\beta = 30$ over a large range in scale, $0.1 \leq \mu/m_H \leq 10$. The higher-order threshold corrections greatly decrease the scale dependence of the cross section. The NNNLO-NLL curve is relatively flat. This can also be demonstrated by calculating at each order the ratio of the maximum value to the minimal value of the cross section over the μ range. We find

$$\sigma_{\max}/\sigma_{\min} = \begin{array}{cccc} 3.39 & 1.50 & 1.38 & 1.32 \\ \uparrow & \uparrow & \uparrow & \uparrow \\ \text{LO} & \text{NLO-NLL} & \text{NNLO-NLL} & \text{NNNLO-NLL} \end{array}$$

We see that with progressing order the ratio decreases and gets closer to one.

In Figure 6 we plot the dependence of the H^- cross section on $\tan\beta$ (left) and the top quark mass (right) with $\mu = m_H = 500$ GeV. The $\tan\beta$ variation in the left plot is over the range $1 \leq \tan\beta \leq 50$, and the cross section is at a minimum near $\tan\beta = 8$. We note that the $\tan\beta$ dependence arises in the factor $m_b^2 \tan^2\beta + m_t^2 \cot^2\beta$, and the $\tan\beta$ shape is the same for all curves. The dependence on $\tan\beta$ is large, spanning two orders of magnitude in the range shown. The dependence of the cross section on the top quark mass is shown in the right plot for $\tan\beta = 30$. For heavier top quark masses the cross section decreases. We see that the dependence is mild so that the current small experimental uncertainties on the top quark mass do not play a major role in the total uncertainty of the charged Higgs production cross section.

3. Other charged Higgs production channels

We briefly discuss some other production channels for charged Higgs production, including associated production with a W boson, and pair production.

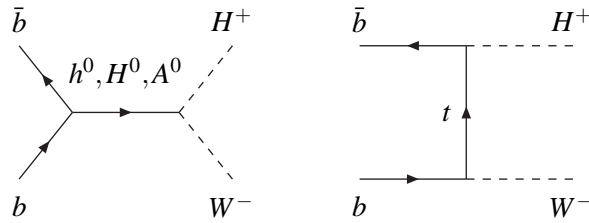


Figure 7: LO diagrams for $b\bar{b} \rightarrow H^+W^-$.

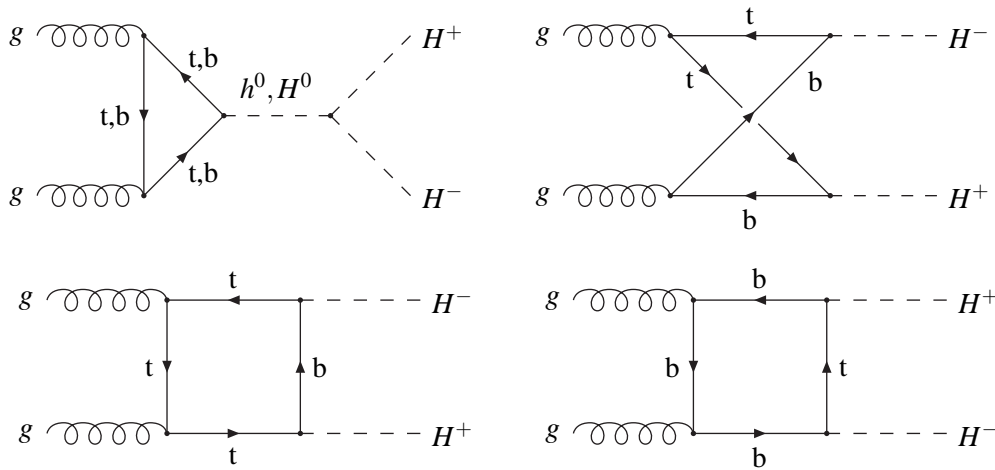


Figure 8: LO diagrams for $gg \rightarrow H^+H^-$.

3.1 Associated H^+ and W^- production

Charged Higgs bosons can be produced in association with W bosons (see, e.g. [5, 6, 20, 21]). The LO processes are $gg \rightarrow H^+W^-$ and $b\bar{b} \rightarrow H^+W^-$. LO diagrams for $b\bar{b} \rightarrow H^+W^-$ are shown in Fig. 7.

Complete NLO calculations for $b\bar{b} \rightarrow H^+W^-$ were presented in [5, 6]. In Ref. [21] the above production process followed by a leptonic decay of H^+ and a hadronic decay of W^- was studied as a possibility for observing charged Higgs bosons at the LHC.

3.2 Charged Higgs pair production

The LO processes for the production of a H^+ , H^- pair are $gg \rightarrow H^+H^-$, $b\bar{b} \rightarrow H^+H^-$, and $q\bar{q} \rightarrow H^+H^-$ with q a light quark.

LO diagrams for $gg \rightarrow H^+H^-$, involving loops with top and bottom quarks, are shown in Figure 8. Studies have been made for charged Higgs pair production via this process at the LHC (see e.g. [22, 23, 24]).

LO diagrams for $b\bar{b} \rightarrow H^+H^-$ are shown in Figure 9. The NLO corrections for this process have been presented in [7, 8]. The NLO corrections for the Drell-Yan type process involving light

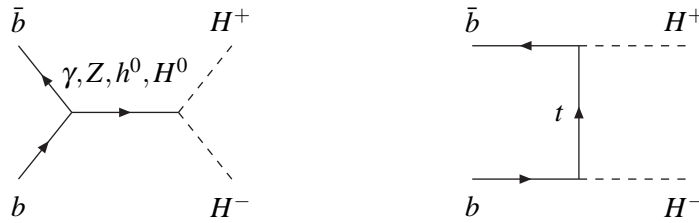


Figure 9: LO diagrams for $b\bar{b} \rightarrow H^+H^-$.

quarks, $q\bar{q} \rightarrow H^+H^-$, were also presented in [8]. At LO the Drell-Yan type process proceeds via an s -channel γ or Z boson, similar to the left diagram of Figure 9.

The relative contribution of the gg , light $q\bar{q}$, and $b\bar{b}$ channels to charged Higgs pair production at the LHC depends on the values of $\tan\beta$ and Higgs mass. At $\tan\beta = 10$ the light $q\bar{q}$ contribution is by far dominant but at $\tan\beta = 50$ the gg contribution dominates [8].

Ref. [25] provides a study of the associated production of a charged Higgs pair with a $b\bar{b}$ pair, $gg \rightarrow b\bar{b}H^+H^-$, which is the dominant pair production mode at large $\tan\beta$ and relevant for the determination of triple-Higgs couplings.

Further calculations of NLO and higher-order corrections will be crucial in reducing uncertainties in the theoretical predictions for cross sections and differential distributions for charged Higgs production.

References

- [1] The Higgs Working Group: Summary Report, *Physics at TeV Colliders* (2003) [hep-ph/0406152].
- [2] S.-H. Zhu, *Phys. Rev. D* 67, 075006 (2003) [hep-ph/0112109].
- [3] T. Plehn, *Phys. Rev. D* 67, 014018 (2003) [hep-ph/0206121].
- [4] E.L. Berger, T. Han, J. Jiang, and T. Plehn, *Phys. Rev. D* 71, 115012 (2005) [hep-ph/0312286].
- [5] W. Hollik and S.-H. Zhu, *Phys. Rev. D* 65, 075015 (2002) [hep-ph/0109103].
- [6] J. Gao, C.S. Li, and Z. Li, *Phys. Rev. D* 77, 014032 (2008), arXiv:0710.0826 [hep-ph].
- [7] H.-S. Hou, W.-G. Ma, R.-Y. Zhang, Y. Jiang, L. Han, and L.-R. Xing, *Phys. Rev. D* 71, 075014 (2005) [hep-ph/0502214].
- [8] A. Alves and T. Plehn, *Phys. Rev. D* 71, 115014 (2005) [hep-ph/0503135].
- [9] N. Kidonakis, *JHEP* 05, 011 (2005) [hep-ph/0412422]; in DIS 2004, p. 951 [hep-ph/0406179]; AIP Conf. Proc. No. 792, 643 (2005) [hep-ph/0505271].
- [10] N. Kidonakis, *Phys. Rev. D* 73, 034001 (2006) [hep-ph/0509079]; PoS (HEP 2005) 336 [hep-ph/0511235].
- [11] L.G. Jin, C.S. Li, R.J. Oakes, and S.H. Zhu, *Eur. Phys. J. C* 14, 91 (2000) [hep-ph/9907482]; *Phys. Rev. D* 62, 053008 (2000) [hep-ph/0003159].

- [12] A. Belyaev, D. Garcia, J. Guasch, and J. Sola, Phys. Rev. D 65, 031701 (2002) [hep-ph/0105053]; JHEP 06, 059 (2002) [hep-ph/0203031].
- [13] G.-P. Gao, G.-R. Lu, Z.-H. Xiong, and J.M. Yang, Phys. Rev. D 66, 015007 (2002) [hep-ph/0202016].
- [14] J.F. Gunion, Phys. Lett. B 322, 125 (1994) [hep-ph/9312201].
- [15] F. Borzumati, J.L. Kneur, and N. Polonsky, Phys. Rev. D 60, 115011 (1999) [hep-ph/9905443].
- [16] S. Moretti and D.P. Roy, Phys. Lett. B 470, 209 (1999) [hep-ph/9909435].
- [17] J. Alwall and J. Rathsman, JHEP 12, 050 (2004) [hep-ph/0409094].
- [18] N. Kidonakis, Int. J. Mod. Phys. A 19, 1793 (2004) [hep-ph/0303186]; in DIS 2003, p. 429 [hep-ph/0307207]; Mod. Phys. Lett. A 19, 405 (2004) [hep-ph/0401147].
- [19] A.D. Martin, R.G. Roberts, W.J. Stirling, and R.S. Thorne, Eur. Phys. J. C 28, 455 (2003) [hep-ph/0211080].
- [20] O. Brein, W. Hollik, and S. Kanemura, Phys. Rev. D 63, 095001 (2001) [hep-ph/0008308].
- [21] D. Eriksson, S. Hesselbach, and J. Rathsman, Eur. Phys. J. C 53, 267 (2008) [hep-ph/0612198].
- [22] A. Krause, T. Plehn, M. Spira, and P.M. Zerwas, Nucl. Phys. B 519, 85 (1998) [hep-ph/9707430].
- [23] Y. Jiang, W.-G. Ma, L. Han, M. Han, and Z.-H. Yu, J. Phys. G 24, 83 (1998) [hep-ph/9708421].
- [24] O. Brein and W. Hollik, Eur. Phys. J. C 13, 175 (2000) [hep-ph/9908529].
- [25] S. Moretti and J. Rathsman, Eur. Phys. J. C 33, 41 (2004) [hep-ph/0308215].